

Synchronous relaxation algorithm for parallel kinetic Monte Carlo

Yunsic Shim* and Jacques G. Amar†

*Department of Physics & Astronomy
University of Toledo, Toledo, OH 43606*

(Dated: March 22, 2022)

We investigate the applicability of the synchronous relaxation (SR) algorithm to parallel kinetic Monte Carlo simulations of simple models of thin-film growth. A variety of techniques for optimizing the parallel efficiency are also presented. We find that the parallel efficiency is determined by three main factors – the calculation overhead due to relaxation iterations to correct boundary events in neighboring processors, the (extreme) fluctuations in the number of events per cycle in each processor, and the overhead due to interprocessor communications. Due to the existence of fluctuations and the requirement of global synchronization, the SR algorithm does not scale, i.e. the parallel efficiency decreases logarithmically as the number of processors increases. The dependence of the parallel efficiency on simulation parameters such as the processor size, domain decomposition geometry, and the ratio D/F of the monomer hopping rate D to the deposition rate F is also discussed.

PACS numbers: 81.15.Aa, 05.10.Ln, 05.10.-a, 89.20.Ff

I. INTRODUCTION

Kinetic Monte Carlo (KMC) is an extremely efficient method^{1,2,3,4,5} to carry out dynamical simulations when the relevant activated atomic-scale processes are known, and KMC simulations have been used to model a variety of dynamical processes ranging from catalysis to thin-film growth. The basic principle of kinetic Monte Carlo is that the probability that a given event will be the next event to occur is proportional to the rate for that event. Since all processes are assumed to be independent Poisson processes, the time of the next event is determined by the total overall rate for all processes, and after each event the rates for all processes are updated as necessary.

In contrast to Metropolis Monte Carlo,⁶ in which each Monte Carlo step corresponds to a configuration-independent time interval and each event is selected randomly but only accepted with a configuration-dependent probability, in kinetic Monte Carlo both the selected event and the time interval between events are configuration-dependent while all attempts are accepted. In the context of traditional Monte Carlo simulations this is sometimes referred to as the n -fold way.¹ While KMC requires additional book-keeping to keep track of the rates of all possible events, the KMC algorithm is typically significantly more efficient than the Metropolis algorithm since no selected moves are rejected. In particular, for problems such as thin-film growth in which the possible rates or probabilities for events can vary by several orders of magnitude, the kinetic Monte Carlo algorithm can be orders of magnitude more efficient than Metropolis Monte Carlo.

Because the attempt time in Metropolis Monte Carlo is independent of system configuration, parallel Metropolis Monte Carlo simulations may be carried out by using an asynchronous “conservative” algorithm.^{7,8,9,10,11} In such an algorithm all processors whose next attempt time is less than their neighbor’s next attempt times are allowed

to proceed. Unfortunately such a “conservative” algorithm does not work for kinetic Monte Carlo since in KMC the event-time depends on the system configuration. In particular, since fast events may “propagate” across processors, the time for an event already executed by a processor may change due to earlier events in nearby processors, thus leading to an incorrect evolution. As a result, the development of efficient parallel algorithms for kinetic Monte Carlo simulations remains a challenging problem.

Lubachevsky has developed⁸ and Korniss et al have implemented¹² a more efficient version of the conservative asynchronous algorithm for parallel dynamical Monte Carlo simulations of the spin-flip Ising model. The basic idea is to apply Metropolis dynamics to events on the boundary of a processor, but to accelerate interior moves by using the n -fold way. The choice of a boundary or interior move is determined by the ratio of the number of boundary sites to the sum of the acceptance probabilities for all interior moves. While all “ n -fold way” interior moves are immediately accepted, all Metropolis attempts must wait until the neighboring processor’s next attempt time is later before being either accepted or rejected. Since such an algorithm is equivalent to the conservative Metropolis Monte Carlo algorithm described above, it is generally scalable,^{9,10,11} and has been found to be relatively efficient in the context of kinetic Ising model simulations in the metastable regime.^{12,13,14}

Recently we have shown¹⁵ that such an approach can be generalized in order to carry out parallel KMC simulations. In this approach, all possible KMC moves are first mapped to Metropolis moves with an acceptance probability for each event given by the rate for that event divided by the fastest possible rate in the KMC simulation. At each stage, the choice of a boundary move versus an interior move is determined by the ratio of a fixed number corresponding to the sum of the rates for all *possible* events which might occur in the boundary

region to the sum of the rates for all existing interior moves. However, because of the possibility of significant rejection of boundary events, the parallel efficiency of such an algorithm can be very low for problems with a wide range of rates for different processes. For example, we have recently¹⁵ used such a mapping to carry out parallel KMC simulations of a simple 2D solid-on-solid “fractal” model of submonolayer growth with a moderate ratio $D/F = 10^5$ of monomer hopping rate D to (per site) deposition rate F . However, due to the existence of significant rejection of boundary events, very low parallel efficiencies were obtained.¹⁵ Furthermore, in order to use such an approach, in general one needs to know in advance *all* the possible events and their rates and then to map them to Metropolis dynamics so that all events may be selected with the appropriate probabilities. While such a mapping may be carried out for the simplest models, for more complicated models it is likely to be prohibitive.

In order to overcome these problems, we have recently proposed a semi-rigorous synchronous sublattice (SL) parallel algorithm¹⁶ in which each processor’s domain is further divided into sublattices in order to avoid a possible conflict between processors. At the beginning of a cycle, one sublattice is randomly selected so that all processors operate on the same sublattice. Each processor then carries out KMC events for the selected sublattice over a time interval which is typically smaller than the inverse of the fastest single-event rate. At the end of each cycle, each processor communicates with its neighboring processors in order to update its boundary region. By carrying out extensive simulations of simple models of thin-film growth we have found that this algorithm leads to a relatively high parallel efficiency and is scalable, i.e. the parallel efficiency is constant as a function of the number of processors N_p . However, for extremely small processor sizes (smaller than a typical diffusion length in epitaxial growth) weak finite-size effects are observed. Thus for problems in which the diffusion length is large or very small processor sizes are required, it may be preferable to use a more rigorous algorithm.

In this paper we discuss the application of a second rigorous algorithm, the synchronous relaxation (SR) algorithm,^{17,18} to kinetic Monte Carlo simulations. This algorithm was originally used by Eick et al¹⁷ to simulate large circuit-switched communication networks. More recently an estimate of its efficiency has been carried out by Lubachevsky and Weiss¹⁸ in the context of Ising model simulations. In the SR algorithm, all processors remain globally synchronized at the beginning and end of a time interval, while an iterative relaxation method is used to correct errors due to neighboring processors’ boundary events. Since this algorithm is rigorous, the cycle length can be tuned to optimize the parallel efficiency and several optimization methods are discussed. However, we find that the requirement of global synchronization leads to a logarithmic increase with increasing processor number in both the relevant fluctuations in the number of

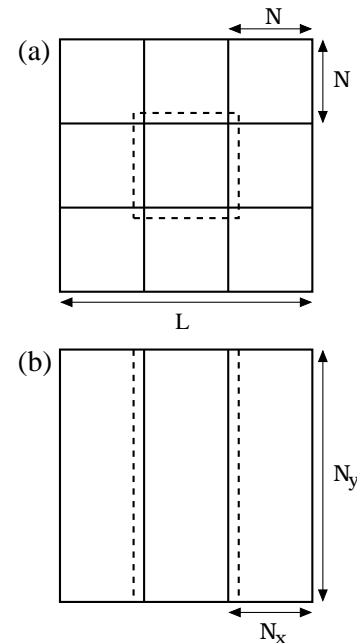


FIG. 1: Schematic diagram of (a) square and (b) strip decompositions. Solid lines correspond to processor domains while dashed lines indicate “ghost-region” surrounding central processor.

events per processor as well as the global communication time. Accordingly, the SR algorithm does not scale since the parallel efficiency decreases logarithmically as the number of processors increases. As a result, the parallel efficiency is generally significantly smaller than for the SL algorithm.

The organization of this paper is as follows. In Section II we describe the algorithm and discuss several different methods of optimization. In Section III we present results obtained using this algorithm for three different models of thin-film growth, along with a brief comparison with serial results. We then discuss the three key factors—number of additional iterations, fluctuations, and communications time—which determine the parallel efficiency of the SR algorithm. The dependence of the parallel efficiency on such parameters as the number of processors as well as the cycle length, processor size, and ratio D/F of monomer hopping rate D to (per site) deposition rate F is also discussed. Finally, in Section IV we summarize our results.

II. SYNCHRONOUS RELAXATION (SR) ALGORITHM

As in previous work on the “conservative” asynchronous algorithm,^{8,9} in the synchronous relaxation (SR) algorithm, different parts of the system are assigned to different processors via spatial decomposition. For the thin-film growth simulations considered here, one may consider two possible methods of spatial decomposition, a

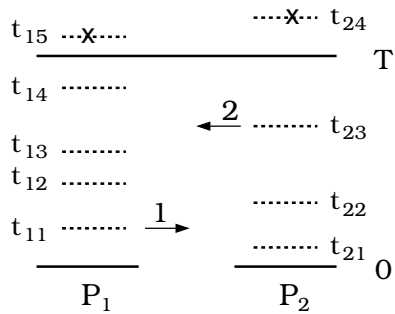


FIG. 2: Diagram showing time evolution in the synchronous relaxation algorithm. Dashed lines correspond to events, while dashed line with an X corresponds to an event which is rejected since it exceeds the time interval T . Arrows indicate boundary events carried out by processors P_1 and P_2 .

square decomposition and a strip decomposition as shown in Fig. 1. Since the square decomposition requires communications with 4 neighbors while the strip decomposition only requires communications with 2 neighbors, we expect that the strip decomposition will have reduced communication overhead. Accordingly, all the results presented here are for the case of strip decomposition. However, as discussed in more detail later, there may be some cases where the square decomposition is preferable.

In order to avoid communicating with processors beyond the nearest-neighbors, the processor size must be larger than the range of interaction (typically only a few lattice units in simulations of thin-film growth). In addition, in order for each processor to calculate its event rates, the configuration in neighboring processors must be known as far as the range of interaction. As a result, in addition to containing the configuration information for its own domain, each processor's array also contains a "ghost-region" which includes the relevant information about the neighboring processor's configuration beyond the processor's boundary.

We now describe the SR algorithm in detail. At the beginning of each cycle corresponding to a time interval T , each processor initializes its time to zero. A first iteration is then performed in which each processor carries out KMC events until the time of the next event exceeds the time interval T as shown in Fig. 2. As in the usual serial KMC, each event is carried out with time increment $\Delta t_i = -\ln(r_i)/R_i$ where r_i is a uniform random number between 0 and 1 and R_i is the total KMC event rate. At the end of each iteration, each processor communicates any boundary events with its neighboring processors, i.e. any events which are in the range of interaction of a neighboring processor and which could thus potentially affect the neighboring processor's event rates and times. Here we define an event as consisting of the lattice sites which have changed due to the event along with the unique time t_i of the event. If at the end of a given iteration, a processor has received any new or missing boundary events (i.e. any boundary events different from those received in the previous iteration)

then that processor must "undo" all of the KMC events which occurred after the time of the earliest new or missing boundary event, and then perform another iteration starting at that point using the new boundary information received. However, if no processors have received new or missing boundary events, then the iterative relaxation is complete, and all processors move on to the next cycle. In order to check for this, a global communications between all processors is performed at the end of each iteration.

In order for the iteration process to converge, one must ensure that within the same cycle the same starting configuration always leads to the same event or transition. Since pseudorandom numbers are used in the KMC simulations considered here, this requires keeping a list of all the random numbers used during that cycle, and backtracking appropriately along the random number list as events are "undone" so that the same random numbers are used for the same configurations. In the ideal implementation described above, events are only redone starting from the earliest new boundary event. However, in the KMC simulations carried out here, lists were used to efficiently select and keep track of all possible events. Since properly undoing such lists is somewhat complex, here we have used a slightly less efficient but simpler method in which every iteration was restarted at the beginning of the cycle. In this case, the necessary changes in the configuration and random numbers were "undone" back to the beginning of the cycle, while the state of the lists at the beginning of the cycle was restored. Since there is significant overhead associated with "undoing" each move, and since in every iteration except the first, one needs to "undo" on average only half of the events in the previous iteration we estimate such a simplification leads to at most a 25% reduction in the parallel efficiency.

We now consider the general dependence of the parallel efficiency on the cycle time T . If the cycle time is too short then there will be a small number of events in each cycle and as a result there will be large fluctuations in the number of events in different processors. This leads to poor utilization, i.e. some processors may process events during a given cycle while others may have very few or no events. In addition, for a short cycle time the communication latency may become comparable to the calculation time which also leads to a reduction in the parallel efficiency. On the other hand, a very long cycle time will lead to a large number of boundary events in each cycle, and as a result the number of relaxation iterations will be large. Thus, in general the cycle length T must be optimized in order to balance out the competing effects of communication latency, fluctuations, and iterations in order to obtain the maximum possible efficiency.

We have used three different methods to control the time interval T in order to optimize the parallel efficiency. In the first method, we have used a fixed cycle length (e.g. $T = \phi/D$ where D is the monomer hopping rate) and then carried out simulations with different values of ϕ in order to determine the optimal cycle length and

maximize the parallel efficiency. In the second method, we have used feedback to dynamically control the cycle length T during a simulation. In particular, every 3 – 10 cycles corresponding to a feedback interval, the elapsed execution time was either calculated or measured, and then used to calculate the ratio ρ (proportional to the parallel efficiency) of the average number of events per cycle n_{av} to the execution time. Based on the values of ρ obtained during the previous two feedback intervals, the cycle length T was adjusted in order to maximize the parallel efficiency. In the third optimization method the cycle length was dynamically controlled in order to attain a pre-determined value for a target quantity such as the number of events per cycle (n_{opt}) or the number of iterations per cycle (n_{it}) whose optimal value was determined in advance. This method turned out to be the most effective since the parallel performance depends strongly on the number of iterations and/or the number of events per cycle. In contrast, while the parallel efficiency obtained using direct feedback was significantly better than that obtained using the first method, it was not quite as good as that obtained using the third method described above. As a result, here we focus mainly on the first and last methods. Unfortunately, both of these methods require the use of additional simulations in order to determine the optimal parameters.

III. RESULTS

In order to test the performance and accuracy of the synchronous relaxation algorithm we have used it to simulate three specific models of thin-film growth. In particular, we have studied three solid-on-solid (SOS) growth models on a square lattice: a “fractal” growth model, an edge-and-corner diffusion (EC) model, and a reversible model with one-bond detachment (“reversible model”). In each of these three models the lattice configuration is represented by a two-dimensional array of heights and periodic boundary conditions are assumed. In the “fractal” model,¹⁹ atoms (monomers) are deposited onto a square lattice with (per site) deposition rate F , diffuse (hop) to nearest-neighbor sites with hopping rate D and attach irreversibly to other monomers or clusters via a nearest-neighbor bond (critical island size of 1). The key parameter is the ratio D/F which is typically much larger than one in epitaxial growth. In this model fractal islands are formed in the submonolayer regime due to the absence of island relaxation. The EC model is the same as the fractal model except that island relaxation is allowed, i.e. atoms which have formed a single nearest-neighbor bond with an island may diffuse along the edge of the island with diffusion rate $D_e = r_e D$ and around island-corners with rate $D_c = r_c D$ (see Fig. 3). Finally, the reversible model is also similar to the fractal model except that atoms with one-bond (edge-atoms) may hop along the step-edge or away from the step with rate $D_1 = r_1 D$, thus allowing both edge-diffusion and

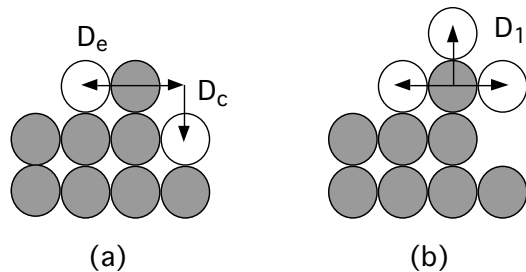


FIG. 3: Schematic diagram of island-relaxation mechanisms for (a) edge-and-corner and (b) reversible models.

single-bond detachment. For atoms hopping up or down a step, an extra Ehrlich-Schwobel barrier to interlayer diffusion²⁰ may also be included. In this model, the critical island size i^{*21} can vary from $i = 1$ for small values of r_1 , to $i = 3$ for sufficiently large values of D/F and r_1 .²²

For the fractal and reversible models, the range of interaction corresponds to one nearest-neighbor (lattice) spacing, while for the EC model it corresponds to the next-nearest-neighbor distance. Thus, for these models the width of the “ghost-region” corresponds to one lattice-spacing. We note that at each step of the simulation, either a particle is deposited or a particle diffuses to a nearest-neighbor or next-nearest-neighbor lattice site. In more general models, for which concerted moves involving several atoms may occur,^{23,24,25,26} the ghost region needs to be at least as large as the range of interaction and/or the largest possible concerted move. In such a case, the processor to which a concerted event belongs can be determined by considering the location of the center-of-mass of the atoms involved in the concerted move.

In order to maximize both the serial and parallel efficiency in our KMC simulations, we have used lists to keep track of all possible events of each type and rate. Each processor maintains a set of lists which contains all possible moves of each type. A binary tree is used to select which type of move will be carried out, while the particular move is then randomly chosen from the list of the selected type. After each move, the lists are updated.

A. Computational Details

In order to test our algorithm we have carried out both “serial emulations” as well as parallel simulations. However, since our main goal is to test the performance and scaling behavior on parallel machines we have primarily focused on direct parallel simulations using the Itanium and AMD clusters at the Ohio Supercomputer Center (OSC) as well as on the Alpha cluster at the Pittsburgh Supercomputer Center (PSC). All of these clusters have fast communications—the Itanium and AMD clusters have Myrinet and the Alphaserer cluster has Quadrics. In our simulations, the interprocessor communications were carried out using MPI (Message-Passing

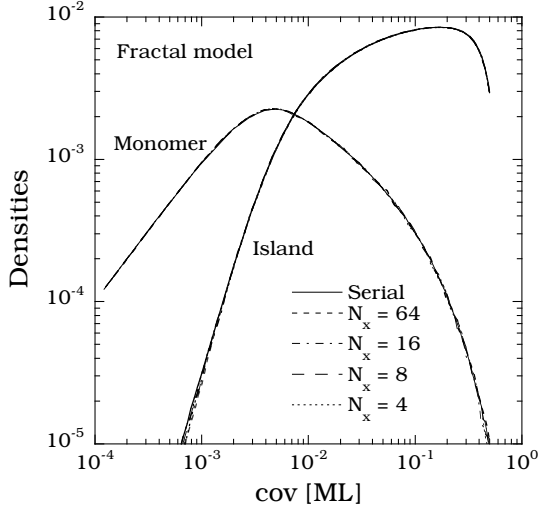


FIG. 4: Comparison between serial and parallel results for the fractal model with $L = 256$ and $D/F = 10^5$.

Interface).

B. Comparison with Serial Results

We first present a brief comparison between serial and parallel results in order to verify the correctness of our implementation of the SR algorithm. Figure 4 shows the monomer and island densities as a function of coverage $\theta \leq 0.5$ for the fractal model with $D/F = 10^5$ and system size $L = 256$ with parallel processor sizes $N_y = 256$ and $N_x = 4, 8, 16$ and 64 corresponding to $N_p = 64, 32, 16$ and 4 respectively (where N_p is the number of processors). As can be seen, there is excellent agreement between the serial and parallel calculations even for $N_x = 4$, the smallest processor size we have tested. Using the SR algorithm, we have also obtained excellent agreement between serial and parallel results for the monomer and island densities for the EC model (not shown).

C. Calculation of parallel efficiency

The parallel efficiency is determined by the competing effects of communication time, fluctuations, and number of relaxation iterations. In particular, the parallel execution time $t_{N_p}(\tau)$ for N_p processors in cycle τ can be written as

$$t_{N_p}(\tau) = t_{calc}(\tau) + t_{com} + t_{other}, \quad (1)$$

where $t_{calc}(\tau)$ and t_{com} denote the calculation and communication time respectively, while the last term t_{other} includes all other timing costs not included in t_{calc} such as sorting boundary events received from neighbors and comparing new boundary events with old ones to see if a new iteration is needed. If there are few boundary events

(as is often the case), then t_{other} may be ignored. The calculation time $t_{calc}(\tau)$ in Eq. 1 may be written as,

$$t_{calc}(\tau) = t_{KMC}^1 \times (n_{av}(\tau) + \Delta(\tau)) \quad (2)$$

where t_{KMC}^1 denotes the average serial calculation time per KMC event, $n_{av}(\tau)$ is the average number of actual events (averaged over all processors) per processor in cycle τ , and $\Delta(\tau)$ corresponds to the additional number of events which must be processed due to fluctuations and relaxation iterations.

Since all processors are synchronized after each iteration, in each iteration the total calculation time is determined by the processor which has the maximum number of events to process. Therefore one may write,

$$\Delta(\tau) = \left(\sum_{j=1}^I [n'_{\max}(\tau, j) + \lambda n'_{\max}(\tau, j-1)] \right) - n_{av}(\tau) \quad (3)$$

where $n'_{\max}(\tau, j)$ is the maximum (over all processors) number of new events in the j th iteration, I is the total number of relaxation iterations, and $\lambda \simeq 0.14$ is a factor which reflects the reduced work to “undo” a KMC event as compared to executing a KMC event. Thus, the parallel efficiency (PE) can be approximated as

$$PE = \frac{t_{1p}}{\langle t_{N_p}(\tau) \rangle} \simeq \left[1 + \frac{\langle \Delta(\tau) \rangle}{n_{av}} + \frac{t_{com}}{t_{1p}} \right]^{-1} \quad (4)$$

where $t_{1p} = n_{av} \times t_{KMC}^1$ is the time for a serial simulation of a single processor’s domain, $n_{av} = \langle n_{av}(\tau) \rangle$, and the brackets denote an average over all cycles. If the communication time is negligible compared to t_{1p} (i.e., $t_{com}/t_{1p} \rightarrow 0$), the maximum possible parallel efficiency can be approximated as

$$PE = \left[1 + \frac{\langle \Delta(\tau) \rangle}{n_{av}} \right]^{-1} \quad (5)$$

We note that $\langle \Delta(\tau) \rangle$ depends primarily on two quantities, the (extreme) fluctuations over all processors in the number of actual events in each cycle $\Delta n^e/n_{av} \equiv (n_{\max} - n_{av})/n_{av}$, and the average number of iterations I per cycle. In particular, one may approximate the additional overhead due to iterations and fluctuations as,

$$\frac{\langle \Delta(\tau) \rangle}{n_{av}} \simeq \eta(I-1)\left(1 + \frac{\Delta n^e}{n_{av}}\right) \quad (6)$$

where a factor of η with $\eta \leq 1$ has been included to take into account the fact that after the first iteration, the number of new events n'_{\max} is typically less than n_{\max} . This result indicates that in the limit of negligible communications overhead, both the average number of iterations per cycle I and the relative fluctuations $\Delta n^e/n_{av}$ should be small in order to maximize the parallel efficiency. We now consider the dependence of each of these quantities on the cycle length T and the number of processors N_p .

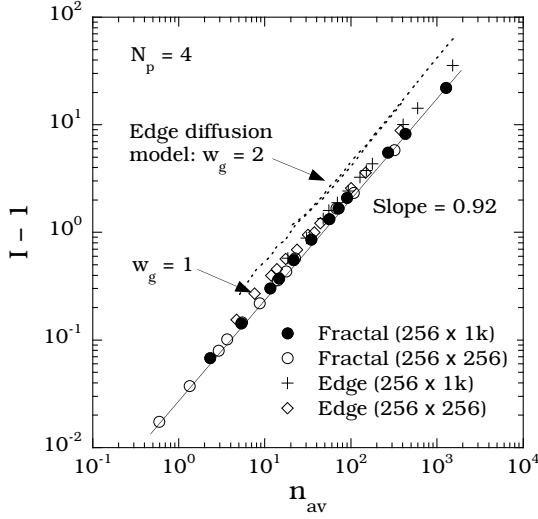


FIG. 5: Number of additional iterations as a function of average number of events per cycle n_{av} with $T = 1/D$. For the EC model $r_e = 0.1$ and $r_c = 0$ are used with $w_g = 1$ and 2 . Here $N_p = 4$ and $\theta = 1$ ML for all cases and $D/F = 10^3 - 10^7$.

D. Number of iterations

Figure 5 shows the number of additional iterations beyond the first iteration $I' = I - 1$ as a function of the average number of events per cycle n_{av} for the fractal and EC models with $N_p = 4$ using strip decomposition and two different processor sizes for different values of D/F . Also shown in Fig. 5 are results for a larger than required ghost-region $w_g = 2$ in order to test the dependence of the number of iterations on the range of interaction. As can be seen, the number of additional iterations is roughly linearly proportional to the average number of events per cycle. Interestingly, for the same average number of events per cycle n_{av} , the number of additional iterations depends relatively weakly on the model, the processor height N_y , and the value of D/F . However, doubling the width of the “ghost” region from $w_g = 1$ to $w_g = 2$ leads to an increase by a factor of approximately 1.5 in the number of iterations.

Figure 6 shows the number of additional iterations I' as a function of the cycle length T for the fractal model with $D/F = 10^5$, $N_p = 4$, and $N_x = 256, N_y = 1024$. As can be seen, the number of additional iterations is roughly but not quite proportional to the cycle length T . Also shown in Fig. 6 is the parallel efficiency, which has been directly measured from the execution time using the definition given in Eq. 4. The maximum parallel efficiency occurs when $T = T_{opt} \simeq 3.0 \times 10^{-6}$ and corresponds to $n_{av} \simeq 30$ KMC events per cycle. We have also calculated (not shown) the optimal cycle length T_{opt} for the same processor size for other values of D/F ranging from 10^3 to 10^7 . While the optimal cycle length varies by approximately two orders of magnitude over this range of D/F , the average optimal number of events per cycle

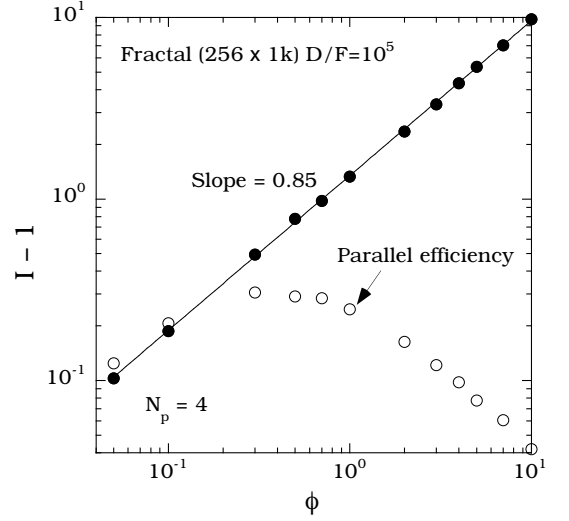


FIG. 6: Number of additional iterations and parallel efficiency for the fractal model as a function of the multiplication factor ϕ with $N_p = 4$, $\theta = 1$ ML and $T = \phi/D$.

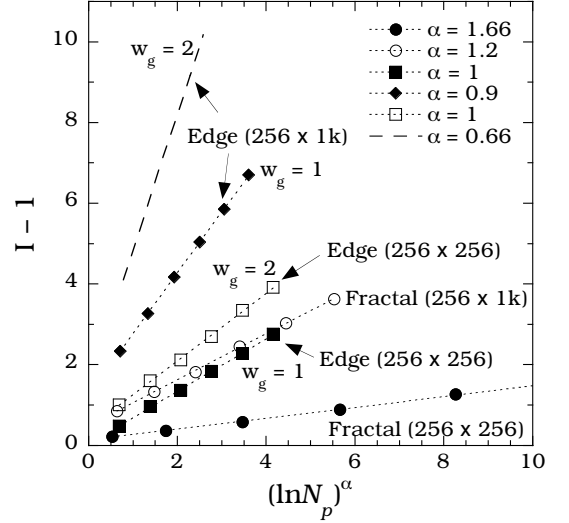


FIG. 7: Number of additional iterations as a function of the number of processors N_p with $2 \leq N_p \leq 64$ for the fractal and edge diffusion models with $D/F = 10^5$, $T = 1/D$ and $\theta = 1$ ML. In the EC model, $r_e = 0.1$ and $r_c = 0$ and the width of the ghost region $w_g = 1$ unless specified.

does not change much— $n_{opt} \simeq 38$ and 30 for $D/F = 10^3$ and 10^7 respectively.

Since the probability of an “extreme” number of boundary events in one of the processors increases with the number of processors for fixed processor size, the number of iterations increases with N_p . As shown in Fig. 7, such an increase is well described by the logarithmic form, $I - 1 = a_0 (\ln N_p)^\alpha$ where the exponent α ranges from 0.66 to 1.7 depending on the model and processor size. Fig. 7 also indicates that an increase of the interaction length from $w_g = 1$ to $w_g = 2$ also yields an approximate doubling in the number of iterations when

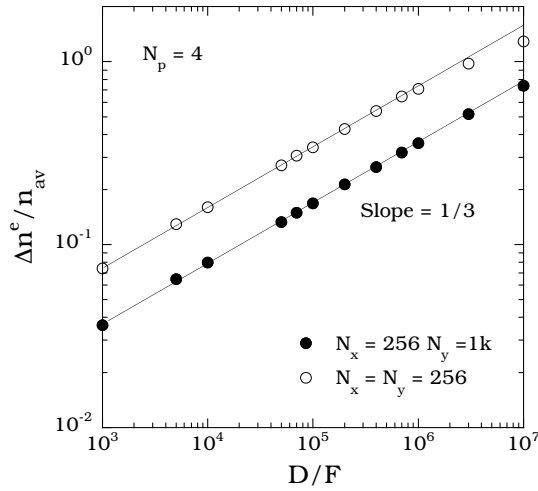


FIG. 8: Relative fluctuation in number of events for the fractal model as a function of D/F with $T = 1/D$, $N_p = 4$ and $\theta = 1$ *ML*.

a fixed time interval $T = 1/D$ is used. Thus, in order to keep the number of iterations constant, the time interval must decrease as the range of interaction increases.

E. Fluctuations in number of events

A second important factor which determines the parallel efficiency is the existence of fluctuations in the number of events in different processors. In particular, since all processors are globally synchronized, the processor having the maximum number of events n_{\max} can determine the execution time of each iteration. Thus the extreme fluctuations $\Delta n^e/n_{av}$, as opposed to the usual r.m.s. fluctuations, determine the parallel efficiency.

Figure 8 shows the measured fluctuations $\Delta n^e/n_{av}$ for the simple fractal model as a function of D/F for fixed processor size $N_x = 256$, $N_y = 1024$ and $N_p = 4$ averaged over many cycles. As expected the relative fluctuations in a smaller system are larger than those in a bigger system. For the simple fractal model, one expects that $n_{av} \sim N_1 \sim (D/F)^{-2/3}$ which implies $\Delta n^e/n_{av} \sim 1/\sqrt{n_{av}} \sim (D/F)^{1/3}$. As can be seen, there is very good agreement with this form for the D/F -dependence.

Figure 9 shows the relative (extreme) fluctuations as a function of the number of processors N_p for the fractal and EC models with two different processor sizes. As for the dependence of the number of iterations on N_p , we find a logarithmic dependence. In particular, we find that $\Delta n^e/n_{av} \sim (\ln N_p)^\gamma$ with $\gamma = 2/3$ regardless of model and processor size. Again, for a fixed N_p , a bigger system shows smaller relative fluctuations than a smaller system. In addition, for the same processor size, the EC model shows smaller relative fluctuations than the fractal model due to the additional number of edge-diffusion events in the model.

We now consider the dependence of the fluctuations

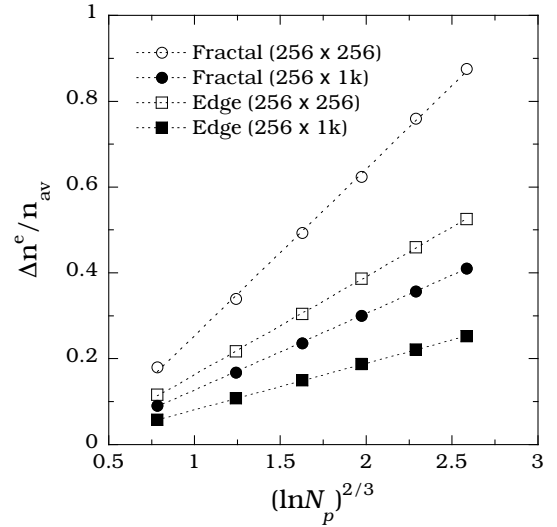


FIG. 9: Relative fluctuation in number of events for fractal and edge diffusion models as a function of number of processors N_p with $D/F = 10^5$, $\theta = 1$ *ML* and $T = 1/D$, where $w_g = 1$ in all cases. In the EC model, $r_e = 0.1$ and $r_c = 0$. Dotted lines are linear fits to data.

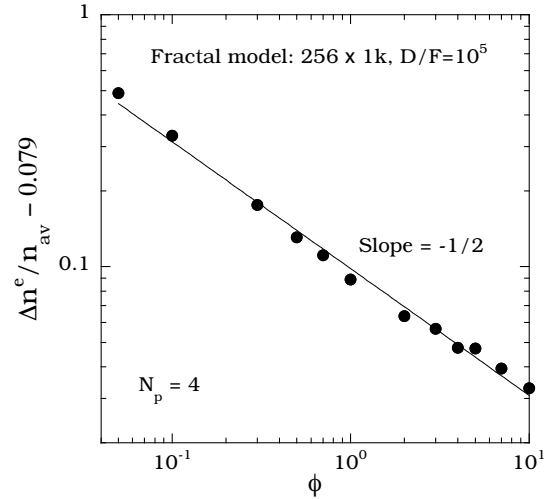


FIG. 10: Power-law decay in the relative fluctuations for the fractal model as a function of multiplication factor ϕ and $T = \phi/D$ with $N_p = 4$ and $\theta = 1$ *ML*.

on the time interval T . For the fractal model, the average number of events per cycle in each processor may be written, $n_{av} = N_x N_y (F + N_1 D) T$ where F is the deposition rate, D is the monomer hopping rate, and N_1 is the monomer density. The fluctuation in the number of events may be written as the sum of the fluctuation (proportional to $n_{av}^{1/2}$) assuming all processors have the same average event rate, and an additional term due to fluctuations in the number of monomers in different processors, i.e. $\Delta n^e \sim n_{av}^{1/2} + N_x N_y \delta N_1^e DT$. We note that the fluctuation $\delta N_1^e = N_1^{\max} - \langle N_1 \rangle$ also depends on the number of processors N_p and the processor size $N_x N_y$.

Dividing to obtain the (extreme) relative fluctuation we obtain,

$$\frac{\Delta n^e}{n_{av}} = \frac{(D/F) \delta N_1^e}{1 + (D/F) \langle N_1 \rangle} + [N_x N_y (F/D + \langle N_1 \rangle) \phi]^{-1/2} \quad (7)$$

where $\phi = DT$. The first term is independent of the cycle length $T = \phi/D$ while for $D/F \gg 1$, $\langle N_1 \rangle \gg F/D$ and so the second term is simply proportional to $\phi^{-1/2}$. As can be seen in Fig. 10, we find good agreement with this form for the fractal model with $N_p = 4$, $D/F = 10^5$, $N_x = 256$, $N_y = 1024$ and the time interval T ranging over more than two decades.

F. Communication time and event optimization

The third factor which determines the parallel efficiency is the communications overhead. For the case of strip decomposition, in every iteration each processor must carry out two local send/receive communications with its neighbors. Typically, a send/receive communication with a small message size (< 100 bytes) between two processors in the same node takes less than $10 \mu s$ but it can take longer if they are in different nodes. For a larger message size the communication overhead increases linearly with message size. Since the processor size in all of our simulations is moderate, the message size is only about 2000 bytes which takes roughly $30 \mu s$.

A global communication (global sum or “AND” and broadcast) must also be carried out at the end of every iteration to check if a new iteration is necessary. The time for the global sum and broadcast is larger than for a local send/receive and increases logarithmically with the number of processors N_p . Overall, we find that the estimated minimum total communication overhead per cycle is roughly $60 \mu s$ for a small number of processors. In comparison, the serial calculation time t_{KMC}^1 for one KMC event is about $5 \mu s$ on the Itanium cluster. Thus, even for a small number of processors the overhead due to communications (t_{com}/t_{1p}) is significant unless $n_{av} \gg 12$.

One way to maximize the parallel efficiency is to use the event optimization method. In this method, the cycle length T is dynamically adjusted during the course of the simulation in order to achieve a fixed target number of events per cycle. By varying the target number of events and measuring the simulation time one may determine the optimal target number n_{opt} . Figure 11 (a) shows the measured parallel efficiency for the fractal model with $N_p = 4$, $N_x = 256$, $N_y = 1024$, and $D/F = 10^5$ as a function of the target number of events. As can be seen, for a target number given by $n_{opt} = 40$ there is an optimal efficiency of approximately 41%. Also shown (dashed line) is the parallel efficiency calculated using the measured additional number of events $\langle \Delta(\tau) \rangle$ due to fluctuations and relaxation iterations along with the estimated communication time which may be approximated by the

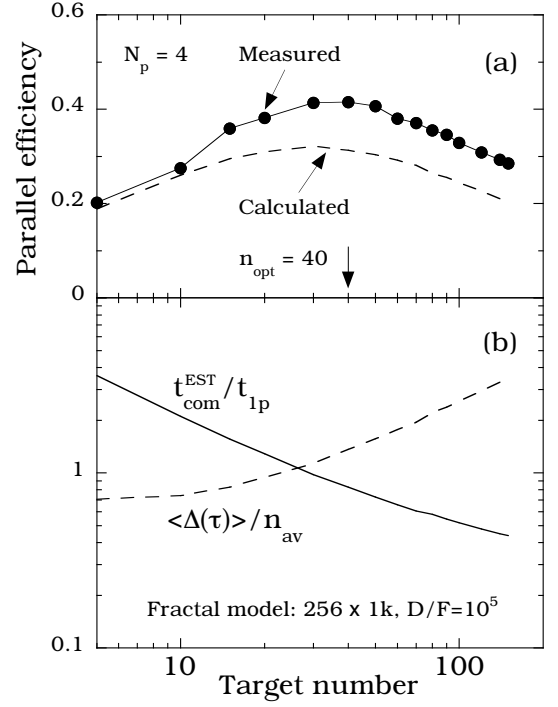


FIG. 11: (a) Parallel efficiency and (b) measured additional number of events and estimated communication time per the average number of events as a function of target number of events with $\theta = 1ML$ and $N_p = 4$.

fit $t_{com}^{est}/t_{1p} \simeq 16I/n_{av}$. The resulting calculated parallel efficiency curve is close to the measured curve but has a slightly lower peak. Fig. 11(b) shows separately the two contributions to the calculated parallel efficiency $\langle \Delta(\tau) \rangle / n_{av}$ and t_{com}/t_{1p} as a function of the target number of events. As can be seen, the peak of the parallel efficiency is close to the point where these two contributions have the same magnitude.

G. Parallel efficiency as a function of D/F

We now consider the parallel efficiency of the SR algorithm as a function of D/F for the fractal model for a fixed number of processors $N_p = 4$. As shown in Fig. 12, when a fixed time interval $T = 1/D$ is used, the parallel efficiency (open symbols) shows a distinct peak as a function of D/F , with a maximum parallel efficiency $PE \simeq 0.3$ for both processor sizes. The existence of such a peak may be explained as follows. For small D/F the PE is low due to the large number of events in each processor which leads to a large number of boundary events and relaxation iterations in each cycle. For large D/F the number of events per cycle is reduced but the communications overhead and fluctuations become significant due to the small number of events. At an intermediate value of D/F which increases with increasing processor size, neither of these effects dominate and the parallel efficiency

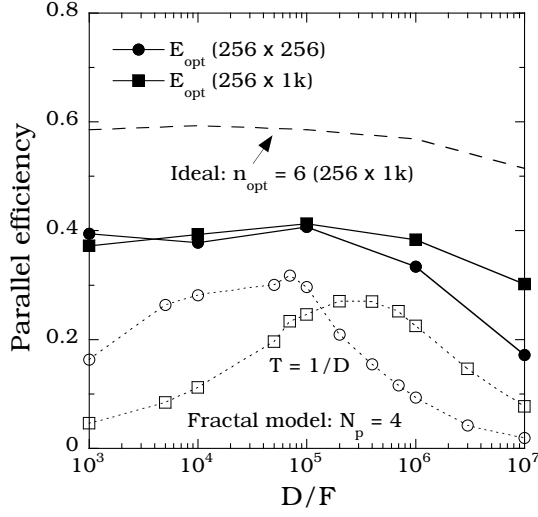


FIG. 12: Parallel efficiency for fractal model as function of D/F with $T = 1/D$ (open symbols) and event optimization (E_{opt}) method (filled symbols). Same symbol shape is used for the same processor size. Here $N_p = 4$ and $\theta = 1$ ML in all cases. In the E_{opt} method, $n_{opt} = 18$ for $N_x = N_y = 256$ and all D/F , and $n_{opt} = 50(40)$ for $N_x = 256, N_y = 1k$ with $D/F < 10^5$ ($\geq 10^5$).

is maximum.

In contrast, when the event optimization method is used (filled symbols) the parallel efficiency is significantly higher and is almost independent of D/F for $D/F \leq 10^6$. Although the value of the optimum target number of events n_{opt} increases with processor size there is only a weak dependence on D/F for fixed processor size. Also shown in Fig. 12 (dashed line) is the estimated ideal parallel efficiency assuming negligible communications overhead. In this case, a small target number of events, $n_{opt} = 6$ was found to yield the maximum ideal parallel efficiency over the range of D/F studied here.

Similar results are shown in Fig. 13 for the edge diffusion model. Since for the edge-diffusion model the “event density” is significantly higher than for the fractal model, the communications overhead and fluctuations are significantly reduced. As a result, for the case of a fixed time interval $T = 1/D$, the maximum parallel efficiency is about 50% for the edge-diffusion model which is significantly higher than the peak value of 30% for the fractal case. When the event optimization method is used, the PE is also higher than for the fractal case and is again roughly independent of D/F . Also shown in Fig. 13 for the larger processor size is the calculated ideal parallel efficiency assuming negligible communications overhead and a target number of events given by $n_{opt} = 6$ (dashed line). Due to the reduced communications overhead for this model, the ideal PE is only slightly higher than the corresponding optimal PE with communications included (filled squares).

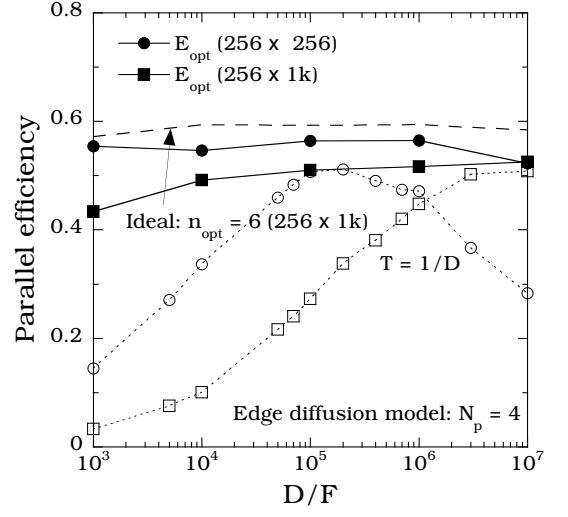


FIG. 13: Parallel efficiency for edge diffusion model as function of D/F with $T = 1/D$ (open symbols) and with event optimization method (filled symbols). Same symbol shape is used for the same processor size. Here, $N_p = 4$, $\theta = 1$ ML , $r_e = 0.1$ and $r_c = 0$. In the E_{opt} method, $n_{opt} = 23(30)$ for $N_x = N_y = 256$ ($N_x = 256$ and $N_y = 1k$) for all D/F . Dashed line represents ideal parallel efficiency $1/[1 + \langle \Delta(\tau) \rangle / n_{av}]$ using $n_{opt} = 6$ with $N_x = 256$ and $N_y = 1k$.

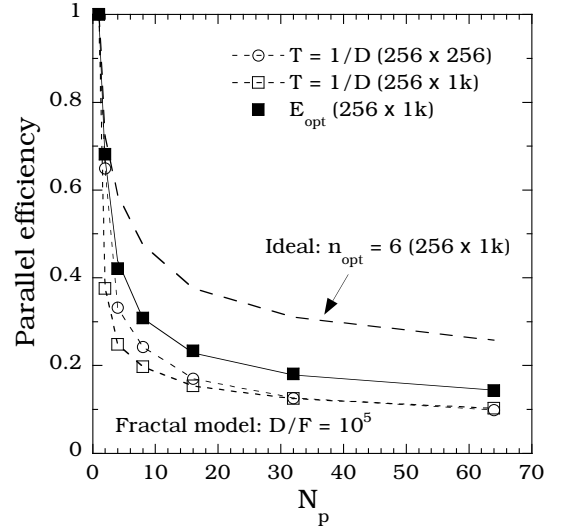


FIG. 14: Parallel efficiency for fractal model with $D/F = 10^5$ as a function of number of processors with $T = 1/D$ (open symbols) and with event optimization method ($n_{opt} = 40$). Dashed line represents ideal parallel efficiency using a target number of events $n_{opt} = 6$. Solid line is a fit to the event-optimization data with a form, $PE = 1/[1 + 0.81(\ln N_p)^{1.4}]$.

H. Parallel efficiency as a function of N_p

We first consider the dependence of the parallel efficiency on the number of processors N_p with fixed processor size. As before, the parallel efficiency is defined as the ratio of the execution time for an ordinary serial simula-

tion of one processor's domain to the parallel execution time of N_p domains using N_p processors (Eq. 4). Fig. 14 shows the parallel efficiency for the fractal model with $D/F = 10^5$ as a function of the number of processors N_p for fixed processor size. Results (open symbols) are shown for two different processor sizes for the case of fixed cycle length $T = 1/D$. Also shown (filled symbols) is the parallel efficiency obtained using event optimization for the larger processor size. While the parallel efficiencies obtained using event optimization are significantly higher than the corresponding results obtained using a fixed time interval, the percentage difference decreases slightly as the number of processors increases.

The solid line in Fig. 14 shows a fit of the form

$$PE = 1/[1 + c (\ln N_p)^\beta] \quad (8)$$

(see Eq. 4) to the parallel efficiency obtained for the larger processor size using event optimization. As can be seen, there is excellent agreement with the simulation results. The value of the exponent ($\beta = 1.4$) is in reasonable agreement with the dependence of the number of additional iterations on N_p shown in Fig. 7. Also shown in Fig. 14 is the ideal parallel efficiency in the absence of communication overhead calculated using a target number of events given by $n_{opt} = 6$. As expected, the ideal PE is significantly larger than the actual PE even for large N_p . In this case a similar fit of the form of Eq. 8 may be made but with $\beta \simeq 1.1$.

Fig. 15 shows similar results for the edge-diffusion model with $D/F = 10^5$, $D_e = 0.1D$ and $D_c = 0$. For the larger processor size ($N_x = 256, N_y = 1024$) both the results obtained using a fixed cycle size and those using event optimization are very similar to the corresponding results already obtained for the fractal model. However, for a fixed cycle length the parallel efficiencies for the smaller processor size ($N_x = N_y = 256$) are somewhat higher than the corresponding results for the fractal model. Again, the ideal parallel efficiency is well described by a fit of the form of Eq. 8 with $\beta \simeq 1.1$. In general, all the parallel efficiencies shown in Figs. 14 and 15 are reasonably well described by fits of the form of Eq. 8 with $0.66 \leq \beta \leq 1.5$.

We now consider the dependence of the parallel efficiency on the number of processors for a fixed total system size L in the case of strip geometry (i.e., $N_y = L$ and $N_x = L/N_p$). Using $L = 1024, D/F = 10^5, E_1 = 0.1$ eV, and a step-edge barrier $E_b = 0.07$ eV at $T = 300$ K, we have carried out multilayer simulations of growth using the reversible model up to a coverage of 10 ML. In this case the parallel efficiency may be written as,

$$PE = \frac{t_{1p}}{N_p t_{av}(N_p)}, \quad (9)$$

where t_{1p} is the calculation time for a serial simulation of the $L \times L$ system. We expect that in this case the parallel efficiency will decrease more rapidly with increasing N_p than for the case of fixed processor size, since the

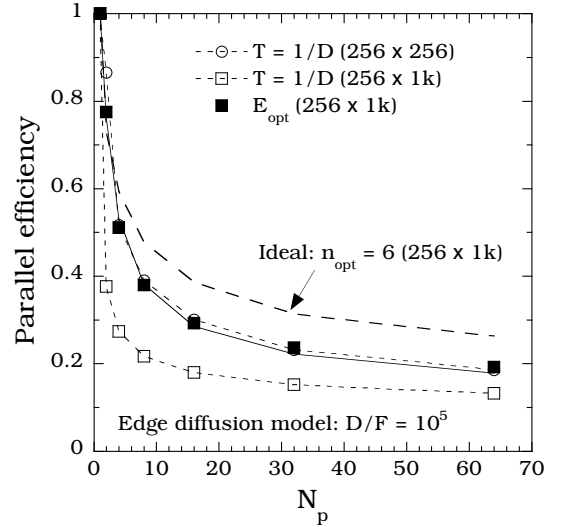


FIG. 15: Parallel efficiency for edge diffusion model with $D/F = 10^5$ as a function of N_p with $T = 1/D$ (open symbols) and with event optimization method ($n_{opt} = 30$). Dashed line represents ideal parallel efficiency obtained using a target number of events given by $n_{opt} = 6$. Solid line is a fit to the data for E_{opt} with a form, $PE = 1/[1 + 0.54(\ln N_p)^{1.5}]$.

decreased processor size leads to increased fluctuations and communications overhead. Using the event optimization method, the parallel efficiencies obtained were 28% ($N_p = 4$), 18% ($N_p = 8$) and 9% ($N_p = 16$), respectively, which corresponds to an approximate N_p^{-1} dependence for the parallel efficiency.

IV. DISCUSSION

We have carried out parallel kinetic Monte Carlo (KMC) simulations of three different simple models of thin-film growth using the synchronous relaxation (SR) algorithm for parallel discrete-event simulation. In particular, we have studied the dependence of the parallel efficiency on the processor size, number of processors, and cycle length T , as well as the ratio D/F of the monomer hopping rate D to the (per site) deposition rate F . A variety of techniques for optimizing the parallel efficiency were also considered. As expected since the SR algorithm is rigorous, excellent agreement was found with serial simulations.

Our results indicate that while reasonable parallel efficiencies may be obtained for a small number of processors, due to the requirement of global communications and the existence of fluctuations, the SR algorithm does not scale, i.e. the parallel efficiency decreases logarithmically as the number of processors increases. In particular, for the fractal and edge-diffusion models with event optimization, we have found that the dependence of the parallel efficiency as a function of N_p may be fit to the form $PE = [1 + c (\ln N_p)^\beta]^{-1}$ where $\beta \simeq 1.5$. If the com-

munication time is negligible compared to the calculation time, then the parallel efficiency is higher but a similar fit is obtained with an exponent close to 1, i.e. $\beta \simeq 1.1$. These results suggest that while the SR algorithm may be reasonably efficient for a moderate number of processors, for a very large number of processors the parallel efficiency may be unacceptably low. These results are also in qualitative agreement with the analysis presented in Ref. 18 that for parallel Ising spin simulations using the SR algorithm with a fixed cycle length, the parallel efficiency should decay as $1/(\log N_p)$ for large N_p .

We have also studied in detail the three main factors which determine the parallel efficiency in the SR algorithm. The first is the extra calculation overhead due to relaxation iterations which are needed to correct boundary events in neighboring processors. As expected, the number of relaxation iterations I' is proportional to the number of boundary events and is also roughly proportional to both the cycle length T and the range of interaction. As a result, decreasing the cycle length will decrease the overhead due to relaxation iterations.

The second main factor determining the parallel efficiency is the relative (extreme) fluctuation $\Delta n^e/n_{av}$ in the number of events over all processors in each iteration. For a fixed number of processors the relative fluctuation decreases as one over the square-root of the number of events per cycle and is thus inversely proportional to the square-root of the product of the processor size and the cycle length. As a result, decreasing the cycle length T will increase the overhead due to fluctuations. However, for a fixed processor size and cycle length the relative fluctuation also increases logarithmically with the number of processors. This increase in the relative fluctuation also leads to an increase in the number of relaxation iterations with increasing N_p as well as decreased processor utilization in each iteration. As a result the parallel efficiency decreases as the number of processors increases.

The third factor determining the parallel efficiency is the overhead due to local and global communications. For the KMC models we have studied the calculation time per event is smaller than the latency time due to local communications. As a result, in our simulations the optimal parallel efficiency was obtained by using a cycle length such that $n_{av} \gg 1$ where n_{av} is the average number of events per processor per cycle. In general, the optimal value of n_{av} may be determined by balancing the overhead due to relaxation iterations and fluctuations with the overhead due to communications. Since the global communications time increases logarithmically with the number of processors, the communications overhead also leads to a decrease in the parallel efficiency with increasing N_p .

In order to optimize the parallel efficiency, we have considered and applied several techniques. These include (i) carrying out several simulations with a different fixed time interval $T = \phi/D$ in order to determine the optimum value of ϕ , (ii) using direct feedback to dynamically control the cycle length during a simulation in order to

maximize the ratio of the average number of events per cycle n_{av} to the measured or estimated execution time, and (iii) using feedback to dynamically control the cycle length in order to obtain a pre-determined “target number” for an auxiliary quantity such as the number of events per cycle or the number of iterations per cycle. While the first two methods are the most direct, we have found that in most cases, the third method results in the highest parallel efficiency. However, since there is no a priori way of knowing the optimal target number in advance, this optimization method must be accompanied by additional simulations.

For the case of negligible communication time, corresponding to simulations in which the calculation time is much longer than the communication time, the cycle time should be small in order to minimize the number of additional iterations but not too small since a very small cycle time will lead to large relative fluctuations. For a processor size $N_x = 256, N_y = 1024$, we found that $n_{opt} \simeq 6$ leads to ideal parallel efficiencies which were significantly larger than obtained using event optimization with the communications time taken into account.

We note that in our simulations we have focused primarily on the case of strip decomposition in order to minimize the communications overhead. However, if the calculation time is significantly larger than the communications time, then for a square system the parallel efficiency may be somewhat larger if a square decomposition is used instead. To illustrate this we consider the decomposition of an L by L system into N_p domains. If the width of the boundary region or range of interaction is given by w , then for the case of strip decomposition the area of the boundary region in each processor is given by $A_{bdy} = 2wL/N_p$. However ignoring corner effects, the area of the boundary region for the square decomposition case is given by $A_{bdy} = 4wL/\sqrt{N_p}$. For $N_p > 4$, the area of the boundary region is smaller for square decomposition than for strip decomposition. Since the number of iterations is roughly proportional to the area of the boundary region, the calculation overhead due to relaxation iterations will be larger for $N_p > 4$ for the case of strip decomposition. As a result, we expect that for a fixed (square) system size and a large number of processors, and for systems (unlike those studied here) with a high ratio of (per event) calculation time to communications time, square decomposition may be significantly more efficient than strip decomposition.

We also note that in our simulations we have used two slightly different definitions for the parallel efficiency. In the first definition (Eq. 4), the parallel execution time was compared with the serial execution time of a system whose size is the same as a single processor. In contrast, in the second definition (Eq. 9) the parallel execution time was directly compared with $1/N_p$ times the serial execution time of a system whose total system size is the same as in the parallel simulation. If the serial KMC calculation time per event is independent of system size, then there should be no difference between the two def-

initions. Since in the models studied here we have used lists for each type of event, we would expect the serial calculation time per event to be independent of system size, and thus the two definitions of parallel efficiency should be equivalent. To test if this is the case, we have calculated the serial simulation time per event for the fractal model for $D/F = 10^3$ and $D/F = 10^5$ for a variety of system sizes ranging from $L = 64$ to $L = 2048$. Somewhat surprisingly, we found that the serial calculation time per event increases slowly with increasing processor size. In particular, an increase of approximately 50% in the calculation time per event was obtained when going from a system of size $L = 64$ to $L = 2048$. We believe that this is most likely due to memory or “cache” effects in our simulations. This increase in the serial calculation time per event with increasing system size indicates that the calculated parallel efficiencies shown in Fig. 14 and Fig. 15 would actually be somewhat larger if the more direct definition of parallel efficiency (Eq. 9) were used.

We now discuss some possible improvements of the method described here. As already noted, in our parallel KMC simulations, lists were used in order to maximize the serial efficiency. However, for simplicity each additional iteration after the first iteration was restarted at the beginning of the cycle rather than starting with the first new boundary event in each processor. By using the more efficient method of only redoing events starting with the first new boundary event, we expect a possible maximum increase in the parallel efficiency of approximately 25% over the results presented here. In addition, it is also possible that by using improved feedback methods, the parallel efficiency may be somewhat further increased. For example, by modifying the feedback

algorithm it may be possible to further improve the direct optimization method. It may also be possible to combine all three optimization methods to obtain an improved parallel efficiency for a given simulation.

Finally, we note that the main reason for the low parallel efficiency for a large number of processors is the global requirement that all processors must be perfectly synchronized. However, for systems with short-range interactions it should be possible to at least temporarily relax this synchronization requirement for processors which are sufficiently far away from one another. Thus, in large systems with a large number of processors it may be possible to increase the parallel efficiency by slightly modifying the SR algorithm by making it somewhat less restrictive. In this connection, we have recently developed¹⁶ a semi-rigorous synchronous sublattice algorithm which yields excellent agreement with serial simulations for all but the smallest processor sizes and in which the asymptotic parallel efficiency is constant with increasing processor number. By combining the synchronous sublattice algorithm with the SR algorithm it may be possible to obtain a hybrid algorithm which contains the best features of both e.g. accuracy and efficiency.

Acknowledgments

This research was supported by the NSF through Grant No. DMR-0219328. We would also like to acknowledge grants of computer time from the Ohio Supercomputer Center (Grant No. PJS0245) and the Pittsburgh Supercomputer center (Grant No. DMR030007JP).

* Electronic address: yshim@physics.utoledo.edu

† Electronic address: jamar@physics.utoledo.edu

- ¹ A. B. Bortz, M.H. Kalos, and J. L. Lebowitz, *J. Comp. Phys.* **17** 10 (1984).
- ² A. F. Voter, *Phys. Rev. B* **34**, 6819 (1986).
- ³ P. A. Maksym, *Semicond. Sci. Technol.* **3**, 594 (1988).
- ⁴ K. A. Fichtorn and W. H. Weinberg, *J. Chem. Phys.* **95**, 1090 (1991).
- ⁵ J. L. Blue, I. Beichl, and F. Sullivan, *Phys. Rev. E* **51**, R867 (1995).
- ⁶ N. C. Metropolis, A. W. Rosenbluth, M. N. Rosenbluth, A. H. Teller, and E. Teller, *J. Chem. Phys.* **21**, 6 (1953).
- ⁷ K. M. Chandy and J. Misra, *IEEE Trans. Software Eng.* **5**, 440 (1979); J. Misra, *ACM Comput. Surv.* **18**, 39 (1986).
- ⁸ B. D. Lubachevsky, *Complex Systems* **1**, 1099 (1987); *J. Comput. Phys.* **75**, 103 (1988).
- ⁹ G. Korniss, Z. Toroczkai, M. A. Novotny, and P. A. Rikvold, *Phys. Rev. Lett.* **84**, 1351 (2000).
- ¹⁰ G. Korniss, M. A. Novotny, Z. Toroczkai, and P. A. Rikvold, in *Computer Simulated Studies in Condensed Matter Physics XIII*, D. P. Landau, S. P. Lewis and H.-B. Schuttler eds. Springer Proceedings in Physics, Vol. 86 (Springer-Verlag, Berlin Heidelberg, 2001).

- ¹¹ G. Korniss, M. A. Novotny, H. Guclu, Z. Toroczkai, and P. A. Rikvold, *Science* **299**, 677 (2003).
- ¹² G. Korniss, M. A. Novotny, and P. A. Rikvold, *J. Comp. Phys.* **153**, 488 (1999).
- ¹³ G. Korniss, C. J. White, P. A. Rikvold, and M. A. Novotny, *Phys. Rev. E* **63**, 016120 (2001).
- ¹⁴ G. Korniss, P. A. Rikvold, and M. A. Novotny, *Phys. Rev. E* **66**, 056127 (2002).
- ¹⁵ Y. Shim and J. G. Amar, unpublished.
- ¹⁶ Y. Shim and J. G. Amar, cond-mat/0406379.
- ¹⁷ S. G. Eick, A. G. Greenberg, B. D. Lubachevsky, and A. Weiss, *ACM Transactions on Modeling and Computer Simulation* **3**, 287 (1993).
- ¹⁸ B. D. Lubachevsky and A. Weiss, in *Proceedings of the 15th Workshop on Parallel and Distributed Simulation* (PADS'01) IEEE (2001). See also <http://arXiv.org/abs/cs.DC/0405053>.
- ¹⁹ J. G. Amar, F. Family, and P.-M. Lam, *Phys. Rev. B* **50**, 8781 (1994).
- ²⁰ G. Ehrlich and F. Hudda, *J. Chem. Phys.* **44**, 1039 (1966); R.L. Schwoebel, *J. Appl. Phys.* **40**, 614 (1969).
- ²¹ J. A. Venables, *Philos. Mag.* **27**, 697 (1973). J. A. Venables, G. D. Spiller, and M. Hanbucken, *Rep. Prog. Phys.* **47**, 399

- (1984).
- ²² J. G. Amar and F. Family, Phys. Rev. Lett. **74**, 2066 (1995).
- ²³ Z.-P. Shi, Z. Zhang, A. K. Swan, and J. F. Wendelken, Phys. Rev. Lett. **76**, 4927 (1996).
- ²⁴ J. C. Hamilton, M. R. Sorensen, and A. F. Voter, Phys. Rev. B **61**, R5125 (2000).
- ²⁵ G. Henkelman and H. Jonsson, Phys. Rev. Lett. **90**, 116101 (2003).
- ²⁶ M. R. Sorensen and A. F. Voter, J. Chem. Phys. **112**, 9599 (2000); A. F. Voter, F. Montalenti, and T. C. Germann, Annu. Rev. Mater. Res. **32**, 321 (2002).